

# Three-dimensional P wave velocity structure of shallow crust beneath the northern Awaji Island derived from refraction seismic explosion

Tomotsugu Demachi<sup>1</sup>, Akiko Hasemi<sup>2</sup>, Takaya Iwasaki<sup>3</sup>, and Mitsuru Onodera<sup>4\*</sup>

<sup>1</sup>Division of Interactive Symbiosphere Sciences, Graduate School of Science and Engineering, Yamagata University, Yamagata 990-8560, Japan

<sup>2</sup>Department of Earth and Environmental Sciences, Faculty of Science, Yamagata University, Yamagata 990-8560, Japan

<sup>3</sup>Earthquake Research Institute, the University of Tokyo, Tokyo 113-0032, Japan

<sup>4</sup>Research Centre for Prediction of Earthquakes and Volcanic Eruptions, Graduate School of Science, Tohoku University, Sendai 980-8578, Japan

(Received September 24, 2003; Revised January 26, 2004; Accepted February 18, 2004)

After the 1995 Hyogo-ken Nanbu (Kobe) earthquake (M7.2), the Research Group for Explosion Seismology (RGES) conducted a refraction seismic experiment in the northern part of the Awaji Island in order to investigate a detailed structure around the source region. In the surveyed area, 145 temporal observation stations were deployed two-dimensionally at 200–250 meters intervals, and 7 shots of 150 kg charges were detonated. Using the first arrival times, we derived a three-dimensional P wave velocity structure of the shallow crust in this region. A dominant feature was the low velocity in the northern part of the region as compared with the southern part. The averages of velocities in the northern area were 4.1 km/s (at a depth of 0.09 km) and 4.5 km/s (at 0.49 km). In the southern region, these were 4.9 and 5.2 km/s, respectively. The study region was mostly within the Cretaceous granitic rocks, and we cannot find a difference in geology that corresponds to the velocity variation. On the other hand, the Bouguer anomaly and the resistivity distributions are consistent with the lateral velocity difference.

**Key words:** Seismic refraction, Hyogo-ken Nanbu (Kobe) earthquake, 3-D velocity, granitic rocks.

## 1. Introduction

So far numerous tomographic studies have been carried out to image the 3-D velocity structure of the crust and upper mantle. However, few tomographic studies have been made for investigating the 3-D velocity variations in the very shallow portion of the crust. A detailed 3-D velocity model of the shallow crust is very important for understanding the depth of the surface geology, and would be very useful for strong-motion earthquake simulation studies.

The Hyogo-ken Nanbu (Kobe) earthquake (M7.2) occurred on January 17, 1995, and brought severe damage to the southern part of the Hyogo Prefecture. After this earthquake, various studies were carried out concerning the structure in and around the source region (e.g. Research Group for Explosion Seismology (RGES), 1997a and 1997b; Kurashimo *et al.*, 1998; Sato *et al.*, 1998; Zhao and Negishi, 1998). RGES conducted a seismic refraction experiment in the northern part of the Awaji Island (RGES, 1997a) (Fig. 1). This experiment deployed 2-D geometry of observation lines within about a 5 km × 10 km region. The study region was almost within the Cretaceous granitic rock body (Fujita and Maeda, 1984; Mizuno *et al.*, 1990) (Fig. 2). The travel time data obtained by this experiment provided information on the lateral structural variation in the granitic rock body near the fault. Piao *et al.* (1996a) analysed the travel times along each

profile line and estimated a 2-D P wave velocity structure down to a depth of 1–2 km for each line, respectively. The result showed that the velocity was much lower in the northern area (4.1–4.3 km/s) than in the southern area (5.2–5.4 km/s). This result is very valuable because there have been few studies concerning velocity variations within a granitic rock body.

Piao *et al.*'s (1996a) study, however, is limited to a 2-D structure in the surveyed area. In order to confirm that such velocity variation exists within the granitic rock body in this region, we have to find out the velocity structure of the whole region by using a tomographic analysis. In the present study, we applied a tomography method developed by Onodera *et al.* (1998), and obtained a 3-D P wave velocity distribution in the northern part of the Awaji Island.

## 2. Data

The core of the Awaji Island mainly consists of Cretaceous granitic rocks. In the middle part of the mountainous area, early to middle Miocene sedimentary rocks (Kobe Group) are overlying these granitic rocks. The early to middle Miocene Kobe group, the Plio-Pleistocene Osaka Group, the late Pleistocene deposits, and alluvium are distributed in the coastal area (Fig. 2). Active faults, the Kusumoto, Higashiura and Nojima faults, run along a coast in a NE-SW direction. These faults are high-angle reverse faults with a right-lateral strike slip component. An earthquake fault appeared along the Nojima fault following the Hyogo-ken Nanbu earthquake (Nakata *et al.*, 1995).

The seismic experiment using explosive shots was conducted on December 14 and 15, 1995, in the northern part

\*Present address: Iwaki Sakuragaoka High School, Iwaki 970-8026, Japan.

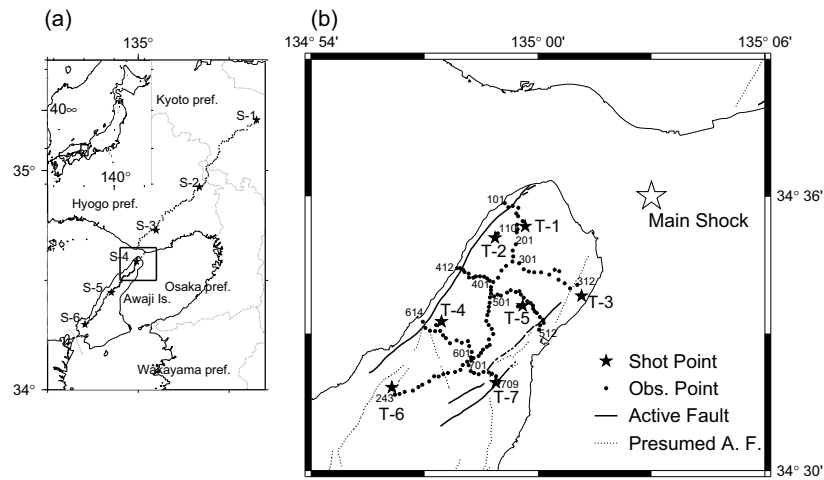


Fig. 1. (a) Location of the study region. Stars and dots indicate shot points and observation sites of the Keihoku-Seidan profile by the RGES (1997b). (b) Locations of shot and observation points used in the present study. Numbers attached to observation sites correspond to those in Fig. 7. The epicentre of the 1995 Hyogo-ken Nanbu Earthquake, active faults and presumed active faults by Nakata and Imaizumi (eds.) (2002) are also shown.

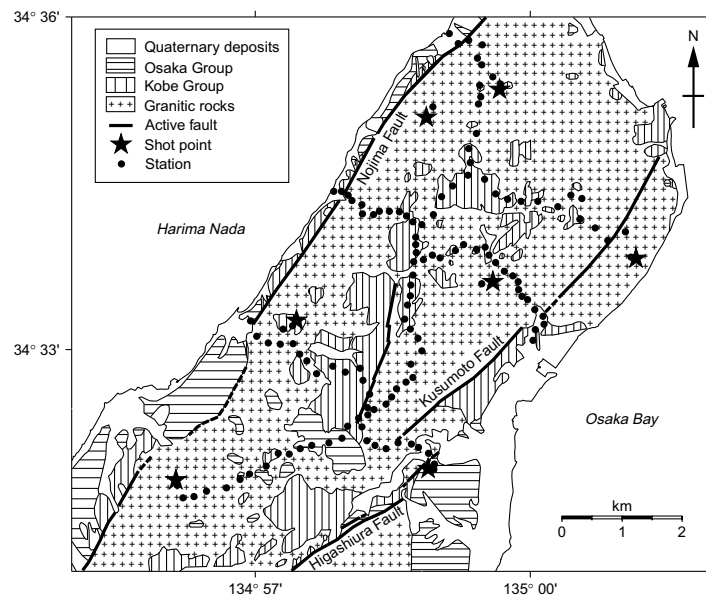


Fig. 2. Geological division of the northern part of the Awaji Island, modified after Fujita and Maeda (1984) and Mizuno *et al.* (1990). Stars and solid circles indicate shot points and observation sites used in the present study.

of Awaji Island (RGES, 1997a). In this experiment, seven shots with a 150 kg-charge, T-1 to T-7, were observed at 145 temporal stations (Figs. 1 and 2). Vertical component seismographs with a natural frequency of 2.2Hz (L22D, Mark Products Co.) were used and seismic signals were recorded by digital recording instruments. A sampling frequency was set at 200 Hz at 133 stations, which formed 2-D observation lines. Twelve stations were densely distributed around the central part of the study region and recorded signals of 100 Hz sampling frequency. We did not use these 12 stations because stations with 200Hz sampling provided enough data concerning the central part of the study region. Five out of 133 stations were located outside Awaji Island, and were excluded from this study. The data analyzed were travel times of first arrivals with a reading uncertainty smaller than 0.03 s. The numbers of stations and travel time data were 128 and 809, respectively. The quality of the record was mostly very

good, and a reading uncertainty was within 0.01s for 85% of the data. Locations of shots and stations used in the present study are shown in Fig. 1.

RGES (1997b) conducted another seismic refraction experiment along the profile line with a length of 135.5 km, extending in a NE-SW direction from Keihoku Town, Kyoto Prefecture, to Seidan Town on Awaji Island, Hyogo Prefecture (Keihoku-Seidan Profile) (Piao *et al.*, 1996b; Ohmura *et al.*, 2001) (Fig. 1(a)). This profile line overlaps the profile line between T-1 and T-6 of the present study.

### 3. P Wave Velocity Model

#### 3.1 Inversion procedure

Onodera *et al.* (1998) developed a computer program for investigating a 3-D velocity structure in a volcanic area using natural earthquake travel time data. The ray-tracing algorithm in this program is based on the finite difference

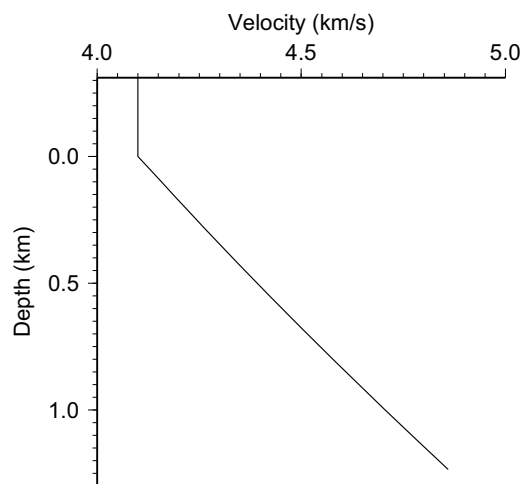


Fig. 3. One-dimensional starting velocity model.

approximation developed by Podvin and Lecomte (1991). This algorithm adopts Huygens' Principle for the determination of ray paths and is suitable for calculating travel times in a highly inhomogeneous velocity structure (Podvin and Lecomte, 1991; Onodera *et al.*, 1998). The observation equation is solved by using the damped least-squares method (Aki and Lee, 1976). We modified this program so that it was applicable for the artificial sources used in the present study.

We modeled a 3-D velocity structure by using a grid, and velocities at grid nodes were obtained by inversion. The interval of nodes was 1.1 km in the N-S and the E-W directions. In the vertical direction, grid nodes were distributed by 0.4 km spacing from 0.31 km above sea level. For calculating travel times, the region was divided into blocks 0.1 km  $\times$  0.1 km  $\times$  0.1 km in size. In the vicinity of a source, the block size should be small in order to reduce the error resulting from the plane wave approximation (Onodera *et al.*, 1998). Therefore, within 1 km from a source, the block size was set to be 0.01 km  $\times$  0.01 km  $\times$  0.01 km. The slowness in each block was calculated by linear interpolation using the velocities at eight grid nodes surrounding the block. We used a 1-D velocity model, shown in Fig. 3, as the initial model. This was derived from Piao *et al.* (1996b). For solving the normal equation, a damping factor which gave a stable solution with a good resolution was determined by trial and error. We used 1% of the largest diagonal element of the coefficient matrix as a damping factor.

Figure 4 shows the result of a checkerboard resolution test (CRT). We alternatively assigned positive and negative velocity perturbations of 5% from the velocity model shown in Fig. 3 to the grid nodes and generated artificial travel times. Station and source combinations and the number of iterations were the same as those for the actual data. From Fig. 4, we can recognize that the checkerboard pattern was almost correctly recovered in the region where the resolution was greater than 0.5.

### 3.2 Result

The velocity model obtained after eight iterations is shown in Figs. 5 and 6. The root mean square (RMS) of travel time residuals was reduced from 0.08 s to 0.02 s. Calculated travel times for the shots T-1 and T-6 are compared with

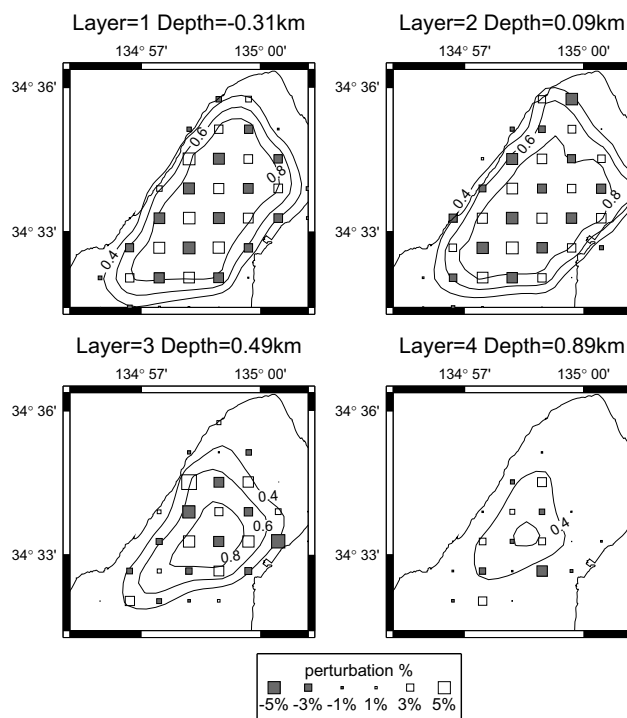


Fig. 4. Results of checkerboard resolution test at the depths of  $-0.31$ ,  $0.09$ ,  $0.49$  and  $0.89$  km. Resolutions are presented by contour lines at an interval of 0.2.

observations in Fig. 7. Though there is a small scatter of observed travel times around the calculated ones, the velocity model explains the observed travel times well.

The velocity distribution reveals lateral structural variations. A dominant feature is low velocities in the northern part of the study region as compared with the southern part. The boundary between the lower and higher velocity areas is located about C-C' line in Fig. 6. Velocities at depths of 0.09 and 0.49 km were obtained with a good resolution. In the area on the north side of the C-C' line, the averages of velocities are 4.1 km/s (at a depth of 0.09 km) and 4.5 km/s (at 0.49 km). In the southern area, these are 4.9 and 5.2 km/s, respectively. The average was taken over the grid nodes with a resolution larger than 0.5. At the depth of 0.09 km, a low velocity area with about 2.1 km/s is distributed near the coast.

A resolution at depth of  $-0.31$  km is lower than that of CRT. This resulted from the difference in the velocity gradient near the Earth's surface. In the obtained model, ray paths are almost vertical near the Earth's surface because of a velocity increase in the vertical direction, and the ray coverage is not good in the shallow depth. On the other hand, in the CRT model, the rays cover a larger area than those of the obtained model, since the velocity gradient near the surface is very small, as shown in Fig. 3.

## 4. Discussion

The prominent features found in Figs. 5 and 6 are the difference between the northern and the southern parts of the region, and low velocities along the coast. These features and the average velocities in the northern and the southern areas are consistent with the result of Piao *et al.* (1996a). The velocity model along the Keihoku-Seidan Profile by Piao *et al.*

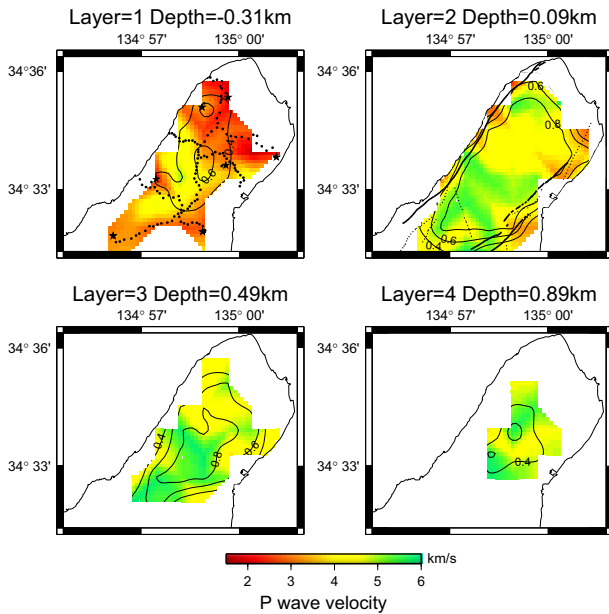


Fig. 5. Three-dimensional velocity model at the depths of  $-0.31$ ,  $0.09$ ,  $0.49$  and  $0.89$  km after eight iterations. Resolutions are presented by contour lines at an interval of  $0.2$ . Shot points and observation sites are shown by stars and dots, respectively, in Layer 1. Solid and broken lines shown in the Layer 2 indicate active faults and presumed active faults, respectively.

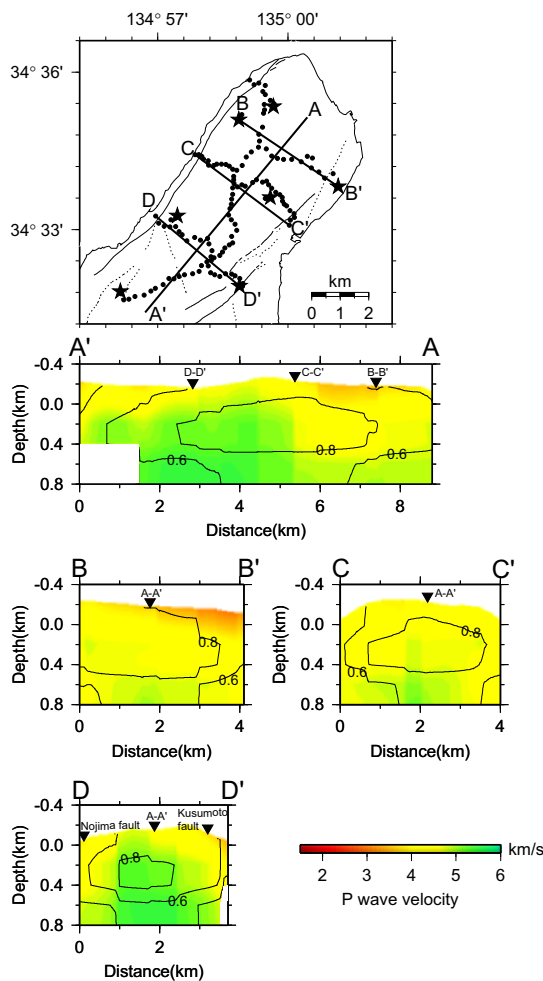


Fig. 6. Vertical cross-sections of A-A', B-B', C-C' and D-D'. Contours indicate resolution at an interval of  $0.2$ . Locations of shot points (stars), observation sites (solid circles), active faults (solid lines) and presumed active faults (broken lines) are shown in the map.

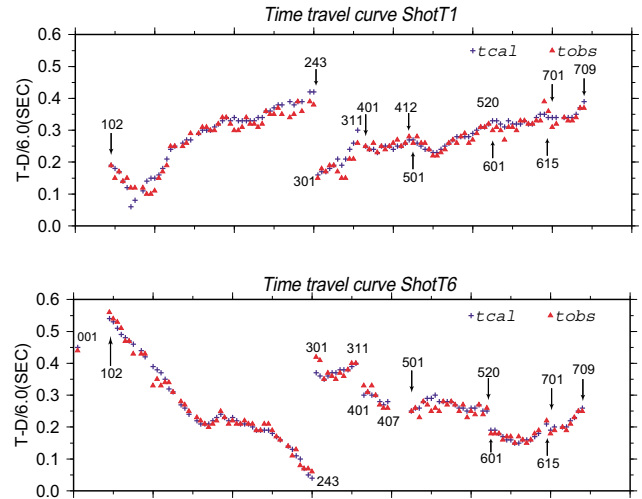


Fig. 7. Travel times for the shots T-1 (upper) and T-6 (lower). Crosses and triangles denote observed and calculated travel times, respectively. Travel times are reduced by  $6.0$  km/s. Numbers correspond to those of observation sites shown in Fig. 1(b).

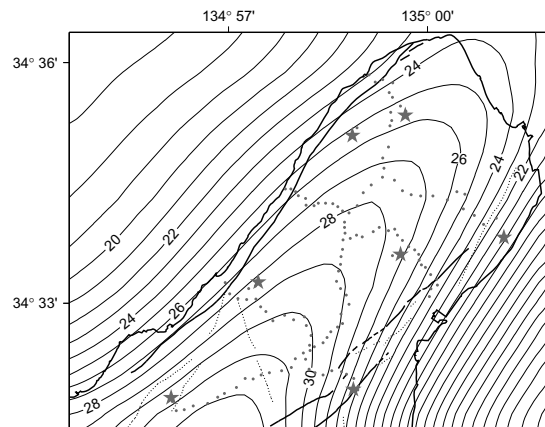


Fig. 8. Bouguer anomaly distributions in the northern part of the Awaji Island (Komazawa, 2000). Contour interval is  $1.0$  mGal. Grey stars and solid circles indicate shot points and observation sites, respectively. Active faults and presumed active faults (Nakata and Imaizumi (eds.), 2002) are shown bold and broken lines.

*al.* (1996b) also showed that the velocity in the northernmost part of the island was lower than the southern area down to a depth of about  $5$  km.

Comparing the velocity distribution with the geology (Fig. 2), low velocities along the coast can be explained by distribution of the Neogene and the Quaternary sediments. However, we cannot find any difference in the geology between the northern and the southern areas that corresponds to the velocity variation.

Here, we compare our result with other geophysical data. The distribution of Bouguer anomalies (Komazawa, 2000) in the vicinity of the study region is shown in Fig. 8. The Bouguer anomalies are small along the coast compared to the inland area. In the inland area, anomalies gradually become higher toward the south. A controlled source audio-magnetotelluric (CSAMT) survey was carried out in almost the same region as the present study (Ikeda *et al.*, 2000). The result obtained for  $0$  km (sea level) showed that the resis-

tivity of the granitic rock body was lower in the northeastern part (200–500  $\Omega$ -m) than in the southwestern part (500–1000  $\Omega$ -m). These features of the Bouguer anomaly and resistivity distribution coincide with the velocity variation. The Bouguer anomaly depends mainly on the density of the rocks, and resistivity depends on some factors such as weathering, alteration and the water content of the rocks. Distribution of these geophysical data implies that the granitic rock body in the northern area is more strongly weathered and has a lower density than the southern area. This may be the main cause of the velocity difference found in the present study.

## 5. Conclusion

An intensive seismic refraction experiment was conducted after the 1995 Hyogo-ken Nanbu earthquake in the northern part of the Awaji Island by RGEs (1997a). Using the first arrival times obtained by this experiment, we derived a 3-D P wave velocity structure of the shallow part of the crust. A ray tracing algorithm based on the finite difference approximation and the damped least-squares method were used in the inversion procedure. The root mean square of the travel time residuals was 0.02 s for the final model. A dominant feature found in the result was that velocities were low in the northern part of the study region as compared with the southern part. The averages of velocities in the northern area were 4.1 km/s (at a depth of 0.09 km) and 4.5 km/s (at 0.49 km). In the southern area, these were 4.9 and 5.2 km/s, respectively. We cannot find the difference in geology that corresponds to the velocity variation, while the Bouguer anomaly and resistivity distributions coincide with our velocity model. Distribution of these geophysical data implies that the granitic rock body in the northern area is more strongly weathered and has a lower density than the southern area. This may be the main cause of the velocity difference found in the present study.

**Acknowledgments.** We would like to thank the Research Group for Explosion Seismology, particularly those members who participated in the experiment. We also would like to thank K. Ito and D. Zhao for their helpful comments, which improved the manuscript. The experiment was conducted by the Fund of the Special Works of the Earthquake Research Institute, University of Tokyo, as one of the disciplines of the Japanese Earthquake Prediction Program. All figures were created using the Generic Mapping Tools (Wessel and Smith, 1998).

## References

- Aki, K. and W. H. K. Lee, Determination of three-dimensional velocity anomalies under a seismic array using first P arrival times from local earthquakes 1. A homogeneous initial model, *J. Geophys. Res.*, **81**, 4381–4399, 1976.
- Fujita, K. and Y. Maeda, Geology of Suma district, Quadrangle series, 1:50,000, Kyoto (11) No. 61, 101 pp., Geological Survey of Japan, Tsukuba, 1984 (in Japanese with English abstract).
- Ikeda, R., Y. Iio, K. Omura, N. Takahashi, Y. Shiokawa, and Y. Matsuda, Active fault investigations by CSAMT and galvanic electric potential logging in the northern part of Awaji Island, Japan, Report of the National Research Institute for Earth Science and Disaster Prevention, **60**, 57–66, 2000 (in Japanese with English abstract).
- Komazawa, M., Gravity grid database of Japan, Gravity CD-ROM of Japan, Digital geoscience map P-2, Geological Survey of Japan, Tsukuba, 2000.
- Kurashimo, E., M. Shinohara, and N. Tsumura, The upper crustal structure in the northern Awaji Island revealed by seismic refraction/wide-angle reflection profiling using vibrators, *J. Seism. Soc. Japan*, **2**, **51**, 233–237, 1998 (in Japanese with English abstract).
- Mizuno, K., H. Hattori, A. Sankawa, and Y. Takahashi, Geology of Akashi district, Quadrangle series, 1:50,000, Okayama (12) No. 83, 90 pp., Geological Survey of Japan, Tsukuba, 1990 (in Japanese with English abstract).
- Nakata, T. and T. Imaizumi (eds.), *Digital Active Fault Map of Japan*, University of Tokyo Press, Tokyo, 2002 (in Japanese).
- Nakata, T., K. Yomogida, J. Odaka, T. Sakamoto, K. Asahi, and N. Chida, Surface fault ruptures associated with the 1995 Hyogoken-Nanbu Earthquake, *J. Geogr.*, **104**, 127–142, 1995 (in Japanese with English abstract).
- Ohmura, T., T. Moriya, C. Piao, T. Iwasaki, T. Yoshii, S. Sakai, T. Takeda, K. Miyashita, F. Yamazaki, K. Ito, A. Yamazaki, Y. Shimada, K. Tashiro, and H. Miyamachi, Crustal structure in and around the region of the 1995 Kobe Earthquake deduced from a wide-angle and refraction seismic exploration, *The Island Arc*, **10**, 215–227, 2001.
- Onodera, M., S. Horiuchi, and A. Hasegawa, Three-dimensional seismic velocity structure in and around the focal area of the 1996 Onikobe Earthquake based on Vp/Vs inversion, *J. Seism. Soc. Japan*, **2**, **51**, 265–279, 1998 (in Japanese with English abstract).
- Piao, C., T. Iwasaki, T. Yoshii, S. Sakai, T. Takeda, T. Moriya, T. Ohmura, K. Miyashita, F. Yamazaki, K. Ito, A. Yamazaki, Y. Shimada, K. Tashiro, and H. Miyamachi, Crustal structure within the source region of the 1995 southern Hyogo prefecture earthquake from high density seismic refraction experiment, *Prog. Abstr. Seism. Soc. Japan*, **2**, B74, 1996a (in Japanese).
- Piao, C., T. Yoshii, T. Iwasaki, S. Sakai, T. Takeda, T. Moriya, T. Ohmura, K. Miyashita, F. Yamazaki, K. Ito, A. Yamazaki, Y. Shimada, K. Tashiro, and H. Miyamachi, Crustal structure in and around the source region of the 1995 southern Hyogo prefectural earthquake deduced from seismic refraction experiment (Keihoku-Seidan profile), *Prog. Abstr. Seism. Soc. Japan*, **2**, B73, 1996b (in Japanese).
- Podvin, P. and I. Lecomte, Finite difference computation of traveltimes in very contrasted velocity models: a massively parallel approach and its associated tools, *Geophys. J. Int.*, **105**, 271–284, 1991.
- Research Group for Explosion Seismology (RGEs), Precise seismic experiment with the use of controlled sources in the vicinity of a fault region of the 1995 Kobe Earthquake within the Awaji Island, *Bull. Earthq. Res. Inst.*, **72**, 119–166, 1997a (in Japanese with English abstract).
- Research Group for Explosion Seismology (RGEs), Seismic refraction experiment in and around a source region of the 1995 Kobe Earthquake (Keihoku-Seidan profile), *Bull. Earthq. Res. Inst.*, **72**, 69–117, 1997b (in Japanese with English abstract).
- Sato, H., H. Hirata, T. Ito, N. Tsumura, and T. Ikawa, Seismic reflection profiling across the seismogenic fault of the 1995 Kobe earthquake, southwestern Japan, *Tectonophysics*, **286**, 19–30, 1998.
- Wessel, P. and W. H. F. Smith, New, improved version of Generic Mapping Tools released, *EOS trans. AGU*, **79**, 579, 1998.
- Zhao, D. and H. Negishi, The 1995 Kobe earthquake: Seismic image of the source zone and its implications for the rupture nucleation, *J. Geophys. Res.*, **103**, 9967–9986, 1998.

T. Demachi (e-mail: sn340@kdw.kj.yamagata-u.ac.jp), A. Hasemi, T. Iwasaki, and M. Onodera